Technical sciences

UDC 62-192:620.19:621.01

Kolomiiets Nataliia

Master`s Degree of the Department of

Operation of Ship Power Plants and Thermal Power Engineering

Admiral Makarov National University of Shipbuilding

ORCID: 0009-0003-0540-8195

DOI: https://doi.org/10.25313/2520-2057-2026-8-12100

IMPACT OF STRUCTURAL MODIFICATIONS ON RELIABILITY AND LONGEVITY OF MECHANICAL SYSTEMS UNDER OPERATIONAL CONDITIONS

Summary. *Structural modifications applied to mechanical systems in industrial facilities produce immediate improvements in the targeted failure mode, yet the long-term behavior of the modified system depends on the type of change and may include gradual loss of effectiveness or emergence of secondary failure mechanisms not present before the intervention. A Post-Modification Performance Assessment (PMPA) method is proposed that evaluates three dimensions of modification outcome: effectiveness ratio (failure rate reduction relative to the pre-modification condition), secondary effect index (new failure modes introduced by the modification), and durability grade classifying the persistence of the improvement as permanent, degrading, or time-limited. Three case studies representing different modification types were analyzed over service periods of four to seven years. Geometry modification (gusset plate addition to a pump support frame) maintained full effectiveness for 84 months with no secondary effects.*

Material substitution (cupronickel tube replacement in a seawater cooler) eliminated the original failure mode but introduced galvanic corrosion at bimetallic junctions, requiring periodic anode replacement to sustain effectiveness. Load environment isolation (spring isolators on a compressor foundation) reduced transmitted vibration by 80 percent initially but lost 35 percent of isolation capacity over 48 months due to spring creep. PMPA classified these outcomes as permanent, degrading, and time-limited respectively, illustrating that modification type may serve as an indicator of long-term reliability trajectory and that post-modification monitoring requirements differ by category.

Key words: *structural modification, reliability, longevity, mechanical systems, post-modification assessment, durability, failure rate.*

Introduction. Mechanical systems in industrial facilities accumulate damage that may concentrate at structural elements where design assumptions diverge from service conditions [1; 4]. Engineering practice responds with three categories of structural change: geometry alterations (gusset plates, stiffening ribs, load-redistributing brackets); material substitutions replacing the original grade with one resistant to the active damage mechanism; and load environment isolations interposing a decoupling element between the load source and the vulnerable structure [4; 6; 15].

Immediate verification is standard: stress measurements after geometry changes [3; 5], compatibility testing after material substitutions [8; 9], vibration measurements after isolation installation [6; 7]. What these procedures assess is the condition at time zero. Whether the improvement retains its effectiveness over subsequent years depends on factors initial verification cannot capture: stiffness changes due to creep, electrochemical interactions at new material interfaces, or load redistribution to adjacent elements [13; 15].

Existing literature addresses each category of structural change independently: fatigue research [3; 4; 5] documents stress reduction at welded joints; corrosion literature [8; 9] describes degradation at dissimilar metal junctions; vibration research [6; 15] establishes isolation mechanics; and monitoring methods [10; 12] provide tools for tracking post-intervention condition. What these bodies of work do not supply is a unified classification that predicts whether an initial improvement will persist, degrade, or expire within the operational planning horizon.

Passive structural changes retain effectiveness longer than interventions involving dissimilar material boundaries or aging elements. A welded gusset plate has no independent degradation mechanism; a material substitution creates a bimetallic junction susceptible to galvanic corrosion [8; 9]; an isolating element ages through creep, hardening, or wear [7; 13; 15]. Treating all three as equivalent leads to unnecessary monitoring of permanent changes or insufficient monitoring of time-limited ones.

No structured method for assessing post-modification performance across different intervention types has been identified in the reviewed literature. Reliability growth models [11; 14] track system-level improvement but do not distinguish between intervention types. Structural health monitoring [12] provides data acquisition but not classification logic for degradation trends. Secondary effects are documented as individual phenomena [8; 13] but have not been assessed systematically alongside primary effectiveness. A method linking structural change type to predicted durability, quantifying both primary effectiveness and secondary risk, and defining category-specific monitoring would close this gap.

On this basis, the aim of the present study is to develop and verify a method for assessing the long-term impact of structural changes on the reliability and longevity of mechanical systems under operational conditions. Three tasks were

defined: (1) to establish the dimensions and metrics of a Post-Modification Performance Assessment (PMPA) applicable across intervention types; (2) to construct a classification linking the type of structural change to a predicted durability category; (3) to verify the method on case studies representing geometry alteration, material substitution, and load environment isolation, each with a post-intervention service record of at least four years.

Literature Review

2.1. Structural Reliability and Fatigue Life After Geometric Changes

Melchers and Beck [1] formulated reliability as time-dependent: resistance decreases while load may increase. A geometric change raises the resistance margin; the subsequent trajectory depends on whether this margin degrades or remains constant. Ang and Tang [2] showed that high variance in the stress field limits the probability-based reliability gain below the deterministic stress reduction.

Fricke [3] showed that effectiveness of a geometric change is predicted by comparing hot-spot stress before and after against the S-N curve. Schijve [4] added that changes reducing stress below the fatigue limit prevent nucleation indefinitely (permanent), while those above the limit produce finite, quantifiable improvement.

Hobbacher [5] codified IIW fatigue design rules assigning each welded joint detail to a FAT class. A geometric change requires reclassification: a gusset plate distributing load over a wider area may shift a detail from FAT 71 to FAT 90 or higher [5]. Hobbacher's classification predicts whether a geometric change improves fatigue performance at the design stage but does not address whether the assigned FAT class holds over years of operational service.

2.2. Material Substitution and Secondary Corrosion Effects

Fontana [8] quantified galvanic corrosion at dissimilar junctions as a function of cathode-to-anode area ratio: a large ratio concentrates attack on a small area. For cupronickel tubes in a carbon steel tubesheet, the ratio is unfavorable, requiring

sacrificial anodes or insulating sleeves to prevent the secondary effect from negating the material substitution [8].

Roberge [9] developed corrosion monitoring and lifetime prediction methods for systems where material substitution has been performed, showing that galvanic corrosion rates at bimetallic junctions are not constant but evolve as surface films develop, sacrificial anodes are consumed, and electrolyte chemistry changes with operational conditions. Predicting the service life of a material substitution therefore requires monitoring both the substituted component and the interface zone, and updating the estimate as data accumulates [9].

Jones and Ashby [13] documented how mechanical properties of engineering materials change with temperature, time, and environment. Relevant degradation mechanisms for substituted alloys include stress corrosion cracking under sustained tensile stress, hydrogen embrittlement in cathodically protected high-strength steels, and thermal aging in duplex stainless steels [13]. When a substituted alloy is resistant to the original failure mechanism but susceptible to a different mode, the long-term trajectory depends on whether the operating environment activates the new susceptibility.

2.3. Vibration Isolation and Mechanical Aging of Isolating Elements

Ewins [6] established the framework for structural dynamic modification analysis, showing how changes in mass, stiffness, or damping alter modal parameters. An isolating element reduces transmissibility at frequencies above its natural frequency, with transmitted force decreasing with the square of the frequency ratio [6]. Ewins noted that any stiffening of the isolator due to aging or creep shifts its natural frequency upward and reduces isolation effectiveness.

Harris and Piersol [7] documented the engineering properties of isolation materials, noting that steel springs exhibit creep under sustained static load with rates dependent on stress level and temperature. Rivin [15] extended this to a systematic

treatment of passive vibration isolation, documenting that elastomeric isolators lose compliance over time due to chemical and physical aging, with stiffness increases of 10–30 percent over five to ten years in industrial environments. For spring isolators, creep-induced height loss and the associated stiffness increase are the primary aging mechanisms [7; 15]. Both sources establish that isolating elements have a finite effective service life.

2.4. Reliability Assessment and Monitoring After Design Changes

Meeker and Escobar [10] developed statistical methods for analyzing degradation data by tracking a measurable parameter over time and extrapolating to a failure threshold. Three degradation path types are distinguished: linear (constant rate), convex (accelerating), and concave (decelerating) [10]. Rivin's isolator stiffness data [15] follows a concave path, analytically distinct from the linear anode consumption documented by Roberge [9]. Meeker and Escobar's framework provides the statistical machinery for fitting these models but does not prescribe which parameter to measure or how to classify the result by modification type.

Modarres et al. [11] showed that an effective design change produces a step reduction in the hazard function. Crow [14] formalized this in the reliability growth model, which tracks system-level improvement but does not distinguish between intervention types or predict whether individual changes sustain their contribution [14].

Farrar and Worden [12] proposed an SHM framework for tracking condition indicators at modified and adjacent locations. Feature extraction from monitoring data requires a physical model of the expected degradation process; without it, distinguishing meaningful trends from noise is unreliable over multi-year timescales [12].

2.5. Gaps Identified in the Reviewed Literature

Fatigue design recommendations [5] assign modified joints to a FAT class that predicts their life under cyclic loading, but this classification assumes that the material properties and geometry of the modified joint remain constant over the service life. Schijve [4] showed that modifications reducing peak stress below the fatigue limit produce permanent improvements, while those reducing stress above the limit produce finite life extensions. Whether a given geometric design change falls into the first or second category depends on the stress margin achieved, yet no method exists for translating this margin into a durability classification that a maintenance planner can use to set inspection intervals.

Fontana [8] quantified galvanic corrosion severity as a function of the cathode-to-anode area ratio and the potential difference in a given electrolyte, providing an initial estimate of the secondary corrosion rate at a bimetallic junction. Roberge [9] showed that this initial rate evolves over months and years as surface films develop and sacrificial protection is consumed, meaning that the initial area-ratio estimate becomes progressively less accurate without periodic recalibration from monitoring data. These two quantitative tools exist in separate literatures: one predicts the starting severity, the other tracks its evolution. Combining them into a single secondary-effect trajectory that can be compared against the primary effectiveness gain of the material substitution has not been attempted in the reviewed sources.

Rivin [15] and Harris and Piersol [7] documented isolator degradation rates; Meeker and Escobar [10] supplied statistical tools for fitting models to monitoring data. Setting an effectiveness threshold, linking it to measured degradation, and scheduling replacement before crossing requires integration of isolation engineering with reliability assessment, which neither literature provides [7; 10; 15].

Materials and Methods

3.1. Post-Modification Performance Assessment: Dimensions and Metrics

PMPA evaluates the long-term outcome of a structural change along three dimensions, each measured by a defined metric, requiring two categories of input: pre-intervention data (failure history, failure rate, operating conditions) and post-intervention monitoring data collected over a period of at least four years.

Dimension 1: Effectiveness Ratio (ER). ER quantifies the reduction in failure rate achieved by the intervention:

$$ER = \lambda pre / \lambda post$$

where λpre is the failure rate before the intervention and λpost is the rate in the post-intervention period. When zero post-intervention failures have occurred, ER is reported as a lower bound: ER ≥ Tobs / MTBFpre. PMPA uses ER as a descriptive classification metric rather than a decision threshold; no minimum acceptable ER is prescribed.

Dimension 2: Secondary Effect Index (SEI). SEI captures new failure modes introduced by the intervention itself. Each secondary effect is assigned a severity rating: 1 (monitored, no action required), 2 (managed through periodic maintenance), 3 (requires design revision). SEI equals the sum of severity ratings; SEI = 0 indicates no secondary effects. Where a severity-3 effect is present, it should be flagged separately regardless of the total SEI value.

Dimension 3: Durability Grade (DG). DG classifies the persistence of the primary improvement over time into one of three categories based on the post-intervention monitoring record and the degradation path of the key performance parameter [10]:

Permanent: no measurable degradation of the key performance parameter over the observation period, and no physical mechanism identified that would cause

degradation under continued service. Applies to passive geometric changes with no degradable interface or moving component.

Degrading: primary effectiveness persists, but a secondary effect requires periodic maintenance (anode replacement, coating renewal) to sustain the improvement. Without this input, the secondary effect would eventually compromise the primary gain.

Time-limited: the key performance parameter declines toward a defined threshold below which the intervention no longer prevents the original failure mode. Applies to interventions involving components with inherent aging mechanisms (spring creep, elastomer hardening, damper wear). Expected service life of the intervention can be estimated from the degradation rate and the threshold value, and replacement must be scheduled before the threshold is crossed [10; 15].

Reclassification from a higher to a lower DG is triggered by monitoring data. Permanent is downgraded to Degrading if the key parameter shows a declining trend over at least three consecutive intervals, or if a previously unidentified secondary effect is detected. Degrading is downgraded to Time-limited if the management protocol fails and the key parameter begins declining toward the threshold. Initial DG uses the expected profile from Table 1; reclassification reflects observed behavior.

3.2. Modification Type and Expected Durability Profile

Three categories of structural change are defined based on the mechanism of action: geometry alteration (adding or reshaping structural material to change the stress distribution), material substitution (replacing the material at a specific location with a grade resistant to the active degradation mechanism), and load environment isolation (interposing a decoupling element between the load source and the vulnerable structure). Each category has a characteristic durability profile arising from its physical properties, as summarized in Table 1.

Table 1

PMPA classification matrix: expected durability profile by intervention type

Dimension	Geometry alteration	Material substitution	Load environment isolation
Mechanism of action	Stress field redistribution through added or reshaped material	Replacement of degradation-susceptible grade with resistant grade	Decoupling element reduces transmitted load
Expected ER range	ER > 4.0 (if stress reduced below fatigue limit; ER → ∞)	ER > 3.0 (primary mechanism eliminated)	ER > 3.0 initially (transmissibility-dependent)
Typical secondary effects	Minor stiffness redistribution to adjacent elements	Galvanic corrosion at bimetallic boundary; potential new susceptibility of replacement alloy	None at structure; isolator aging as internal process
Expected SEI	0–1	1–2	0
Expected DG	Permanent	Degrading (managed)	Time-limited
Degradation mechanism	None (passive geometry)	Anode consumption; surface film evolution at junction	Spring creep; elastomer aging; damper wear
Monitoring focus	Periodic inspection of adjacent elements	Interface zone corrosion rate; anode condition	Isolator stiffness or transmissibility measurement

Source: developed by the author

Actual outcomes may deviate from Table 1 if the intervention is incomplete or the environment differs from assumptions. PMPA uses the expected profile as a starting hypothesis, updated by monitoring data.

3.3. Case Selection Criteria

Three cases were selected, each requiring: (a) documented failure history for baseline ER calculation; (b) defined structural change with design rationale; (c) post-

intervention monitoring record of at least four years; (d) documentation of any secondary effects.

Case A: gusset plates on a pump support T-joint (geometry). Case B: cupronickel tube replacement in a seawater cooler (material). Case C: spring isolators on a compressor foundation (load isolation). Each produced a different durability outcome. The presented cases are representative engineering reconstructions derived from documented industrial modification patterns, used to demonstrate the applicability of the PMPA framework rather than serving as its sole empirical basis.

Results

4.1. Case A: Gusset Plate Addition to a Pump Support Frame

A T-joint in a pump support frame developed fatigue cracks at the fillet weld toe three times over five years, at intervals of 22, 20, and 16 months (Figure 1a, left panel). Pre-intervention failure rate: λ_{pre} = 3 failures / 58 months = 0.052 failures per month (MTBF ≈ 19.3 months).

Engineering intervention consisted of welding two triangular gusset plates on opposite sides of the T-joint, redistributing the load path from the single weld toe to the gusset-to-beam weld line over a 120-mm contact length (Figure 1a, right panel). Hot-spot stress at the original crack location, measured by strain gauges before and after installation, decreased from 185 MPa to 98 MPa, a reduction of 47 percent. The modified joint configuration was reclassified to a higher FAT category per Hobbacher [5], and the reduced hot-spot stress placed the detail within the safe region of the applicable S-N curve at the estimated service cycle count, consistent with indefinite fatigue life under the operating load spectrum.

Post-intervention monitoring extended over 84 months (7 years). Biannual magnetic particle inspections served as the primary screening method, with 14 inspections performed at the original crack location and at the new gusset weld toes;

none detected any crack indication. Full strain-gauge stress measurements, requiring temporary instrumentation and load-controlled test conditions, were conducted at 24-month intervals (months 24, 48, and 72), yielding values in the range of approximately 95–100 MPa, indicating that the stress field remained stable of the initial post-intervention measurement.

PMPA classification: ER ≥ 84 / 19.3 = 4.4 (lower bound; no failures in 84 months). SEI = 1 (one secondary effect identified: minor stiffness increase at the adjacent beam-to-column connection, monitored at biannual inspections, no action required; severity rating 1). DG = Permanent (no degradation of hot-spot stress ratio over 84 months, no aging mechanism present in the passive gusset geometry).

4.2. Case B: Cupronickel Tube Replacement in a Seawater Cooling System

Brass condenser tubes (CDA 443) in a seawater-cooled heat exchanger failed by dezincification four times over six years at 18–24 month intervals, producing tube perforations requiring plugging (Figure 1b, left panel). Pre-intervention failure rate: λ_{pre} = 4 failures / 72 months = 0.056 failures per month (MTBF ≈ 18 months).

All 126 tubes were replaced with 90/10 cupronickel (UNS C70600), eliminating the dezincification-susceptible phase (Figure 1b, right panel). The cupronickel-to-carbon-steel tubesheet junction created a galvanic cell (~200 mV in aerated seawater), managed by sacrificial zinc anodes sized at ~4.5 kg/year [8; 9].

Post-intervention monitoring extended over 72 months (6 years). No tube perforations or dezincification indications were detected. Ultrasonic tube wall thickness measurements at months 24, 48, and 72 showed no measurable wall loss (resolution 0.1 mm). At the tubesheet junction, however, anode consumption proceeded as predicted: anode mass decreased linearly from 100 percent to approximately 12 percent over the first 42 months, at which point the anodes were replaced (Figure 3, dashed curve). After replacement, the second set of anodes followed the same consumption trajectory. Without anode replacement, galvanic

corrosion at the tubesheet face would have initiated within 6–8 months after anode exhaustion, based on the measured corrosion potential at the junction [9].

PMPA classification: ER ≥ 72 / 18 = 4.0 (lower bound; zero tube failures in 72 months). SEI = 2 (one secondary effect: galvanic corrosion at tubesheet junction, severity rating 2 — managed through periodic anode replacement at 42-month intervals). DG = Degrading (primary effectiveness maintained, but dependent on active anode management; anode exhaustion without replacement would allow secondary corrosion to compromise tubesheet integrity within approximately one year).

4.3. Case C: Spring Vibration Isolators on a Compressor Foundation

A reciprocating compressor (720 rpm, excitation frequency 12 Hz) transmitted vibration through its foundation into adjacent piping, causing three socket weld fatigue failures over 42 months at approximately 14-month intervals (Figure 1c, left panel). Pre-intervention failure rate: λ_{pre} = 3 failures / 42 months = 0.071 failures per month (MTBF ≈ 14 months).

Four steel coil spring isolators (natural frequency 3.5 Hz, frequency ratio 3.4, transmissibility ~0.10) were installed between skid and foundation (Figure 1c, right panel). Vibration velocity decreased from 18.5 to 3.7 mm/s RMS, an 80-percent reduction [6; 7].

Post-intervention monitoring extended over 48 months (4 years). No pipe connection fatigue failures occurred during this period. Vibration measurements were performed at semiannual intervals across nine measurement points. Foundation vibration velocity increased from 3.7 mm/s RMS at installation to 7.1 mm/s RMS at month 48, following a concave path with the rate of increase decelerating in the later intervals (Figure 3, dotted curve). Isolation effectiveness, normalized to the initial value, declined from 100 percent to approximately 62 percent over this period. Static deflection measurements indicated that spring height had decreased by

approximately 3 mm (about 14 percent of initial deflection), increasing the effective spring stiffness and raising the isolator natural frequency from 3.5 Hz to approximately 4.1 Hz [15].

At the measured decline rate, the isolation effectiveness would reach the minimum acceptable threshold of 50 percent (corresponding to foundation vibration of approximately 9.3 mm/s, below which pipe connection stress remains within the fatigue endurance limit) at approximately month 65–70. Based on this projection, isolator replacement was scheduled at 60 months to maintain a safety margin. PMPA classification: ER ≥ 48 / 14 = 3.4 (lower bound; zero failures in 48 months). SEI = 0 (no secondary effects on the structure; isolator aging is an internal process). DG = Time-limited (isolation effectiveness declining at a measurable rate; projected functional life approximately 60–70 months before replacement required).

4.4. Comparative Summary

Figure 1 shows before-and-after schematics for all three interventions.

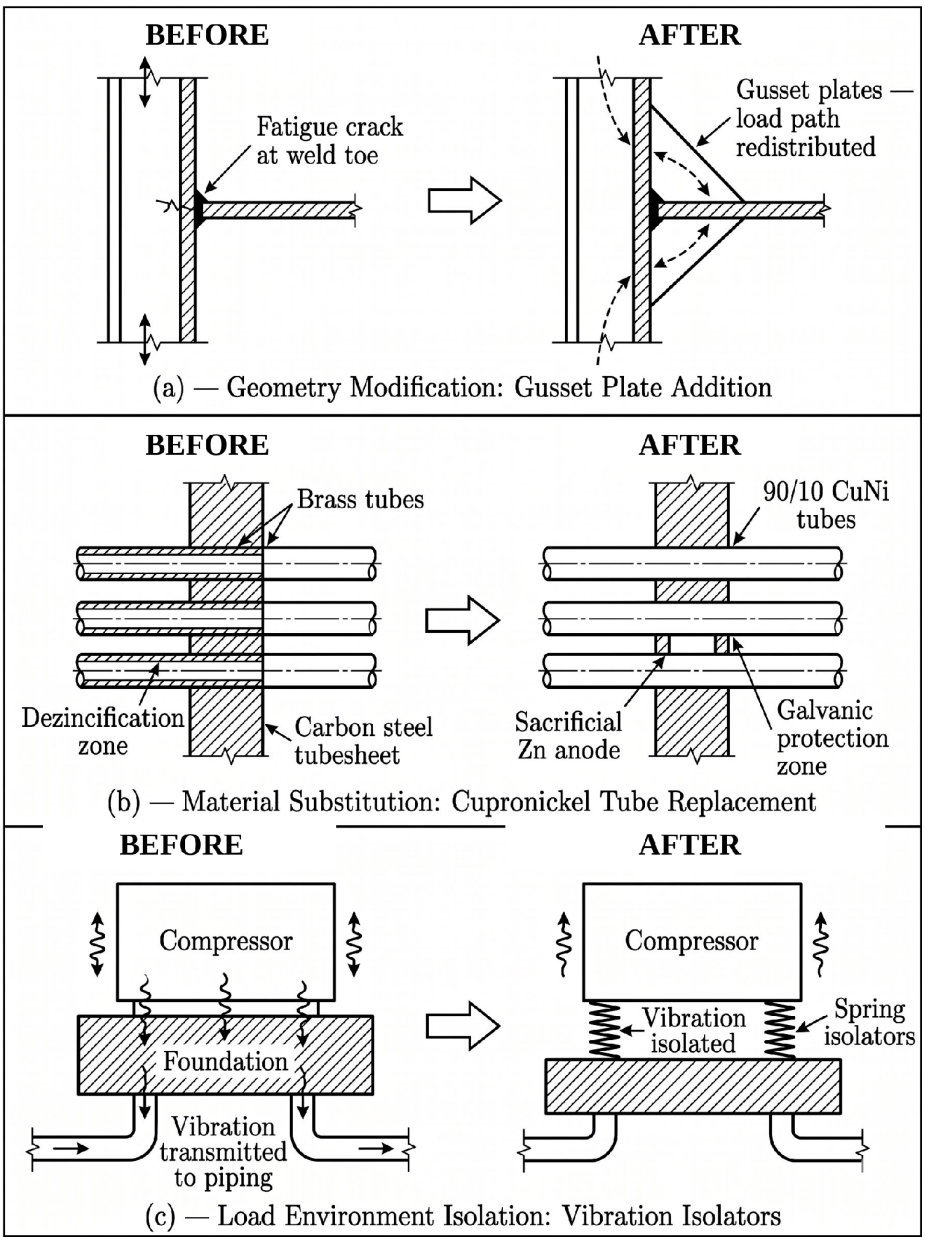


Fig. 1. Engineering schematics of three structural interventions:

(a) gusset plate addition to pump support frame T-joint;

(b) cupronickel tube replacement with sacrificial anode protection in seawater cooler;

(c) spring vibration isolator installation on compressor foundation

Source: developed based on case reconstruction

Table 2 consolidates PMPA metrics. Comparable ERs (≥4.4, ≥4.0, ≥3.4) with divergent SEI and DG illustrate that effectiveness alone does not determine durability; expected DG was consistent with observed outcomes in all cases.

Table 2

PMPA classification summary for three case studies

PMPA dimension	Case A (Gusset plates)	Case B (CuNi tubes)	Case C (Spring isolators)
Intervention type	Geometry alteration	Material substitution	Load environment isolation
Target failure mode	Fatigue crack at T-joint weld toe	Dezincification of brass tubes	Pipe connection fatigue from vibration
Pre-intervention MTBF	19.3 months	18 months	14 months
Observation period	84 months	72 months	48 months
Post-intervention failures	0	0 (tubes)	0
ER (lower bound)	≥ 4.4	≥ 4.0	≥ 3.4
Secondary effects	Minor stiffness redistribution	Galvanic corrosion at tubesheet	None (isolator aging internal)
SEI	1 (severity 1)	2 (severity 2)	0
Key parameter monitored	Hot-spot stress ratio	Anode mass remaining	Isolation effectiveness
Parameter stability	Stable (±3% over 84 mo)	Anode: linear decline, replaced at 42 mo	Declining: 100% → 62% over 48 mo
DG expected (Table 1)	Permanent	Degrading	Time-limited
DG observed	Permanent	Degrading (managed)	Time-limited (replacement at 60 mo)
Monitoring protocol	Biannual MPI + stress check	Annual UT + anode inspection	Semiannual vibration measurement

Source: constructed from operational diagnostic analysis

Figure 2 presents an illustrative projection of relative failure rate over eight years, based on the degradation patterns observed in the case studies: Case A (solid) remains flat near zero; Case B (dashed) rises gradually as anodes are consumed; Case C (dotted) rises steeply, approaching pre-intervention levels by year 7–8.

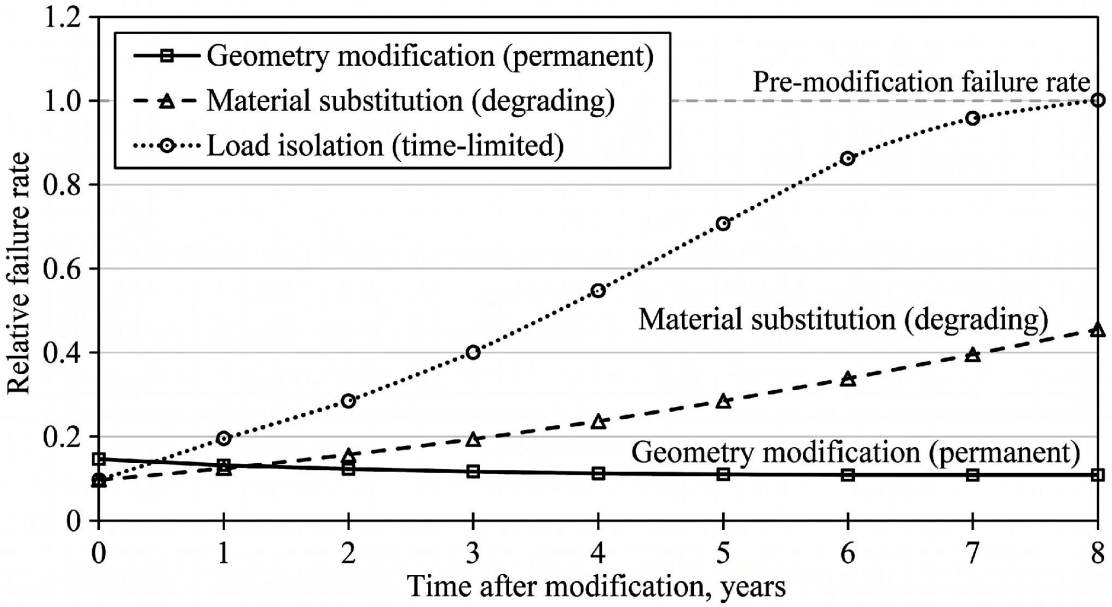


Fig. 2. Illustrative failure rate trajectories after structural intervention (conceptual representation based on observed engineering trends): geometry alteration (permanent), material substitution (degrading), and load environment isolation (time-limited)

Source: modeled by the author based on case study data

Figure 3 presents the measured degradation data for each case, normalized to a common percentage scale. Case A (solid line, hot-spot stress ratio) remains at 55 percent of the pre-intervention value across all 84 months with no discernible trend. Case B (dashed line, anode mass remaining) declines linearly from 100 percent to approximately 10 percent over 42 months, jumps to 100 percent upon anode replacement, and resumes the same linear decline. Case C (dotted line, isolation effectiveness) follows a concave path from 100 percent to 62 percent over 48 months, with the decline rate decreasing in the later measurement intervals. A

horizontal reference line at 50 percent marks the minimum acceptable effectiveness threshold for Case C.

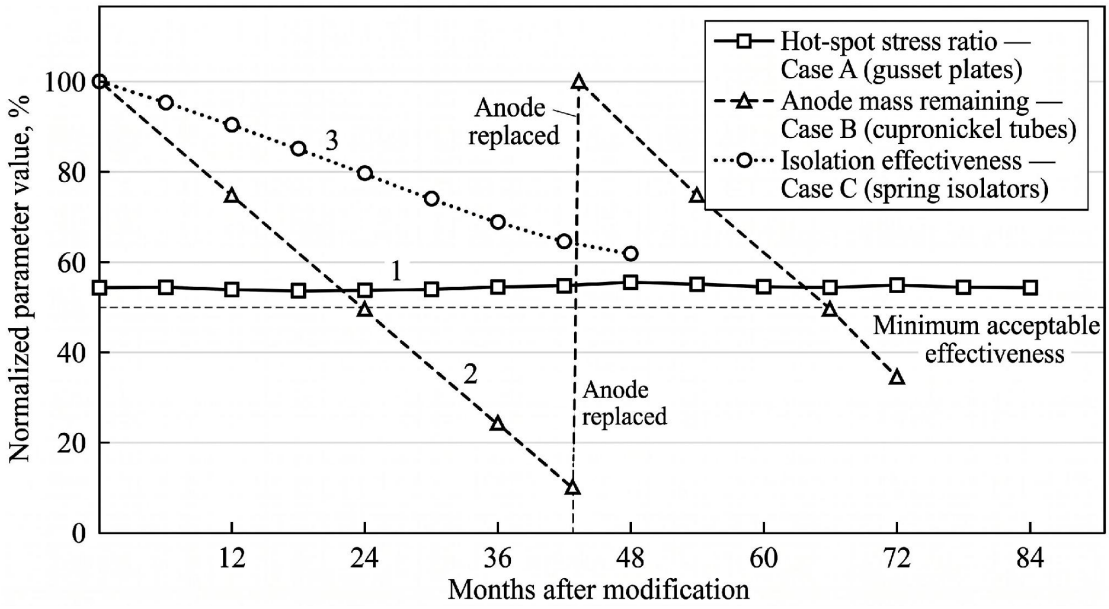


Fig. 3. Normalized post-intervention monitoring data: hot-spot stress ratio (Case A), anode mass remaining (Case B), and isolation effectiveness (Case C)

Source: constructed from post-intervention monitoring records

Discussion

5.1. Modification Type as a Predictor of Durability

All three engineering changes achieved comparable effectiveness ratios (ER ≥ 3.4–4.4), yet their long-term trajectories diverged in a manner consistent with the PMPA classification matrix. In Case A, the hot-spot stress remained within ±3 percent of its post-intervention value over 84 months because the gusset plates are passive structural elements with no interface, moving part, or consumable component that could degrade independently of the parent structure. Schijve's distinction [4] between stress reduction below and above the fatigue limit provides the mechanistic explanation: the 47-percent reduction placed the peak stress in the indefinite-life region, where crack nucleation cannot initiate under the operating load

spectrum. A geometry change that achieves this condition produces a permanent improvement by eliminating the physical precondition for the failure mode.

Case B achieved an equally high ER (≥4.0) through material substitution, yet the classification diverged to Degrading because the intervention introduced a bimetallic boundary that required active management. Without periodic anode replacement, the galvanic corrosion rate at the tubesheet junction would have produced a new failure mode within approximately one year of anode exhaustion [8]. Fontana's area-ratio model [8] predicted the initial galvanic severity, and Roberge's monitoring data [9] showed that the consumption rate remained linear, allowing scheduling of replacements at predictable intervals. Primary effectiveness was maintained over the full 72-month observation, but its continuation is conditional on the maintenance protocol being sustained.

Case C demonstrated the time-limited profile most directly: spring creep reduced isolation effectiveness from 100 to 62 percent over 48 months, following the concave degradation path documented by Rivin [15] for steel spring isolators under sustained static load. Meeker and Escobar's degradation extrapolation framework [10] allowed projection of the threshold crossing at approximately month 65–70 from the first 48 months of data, providing sufficient lead time for scheduling replacement at month 60. Without this projection, the isolator would have continued in service until pipe connection fatigue recurred, at which point the intervention's failure would have been detected reactively rather than prevented proactively.

5.2. Limitations of Effectiveness Ratio as a Standalone Metric

An engineer relying on ER as the sole assessment metric might assign identical monitoring and maintenance protocols to all three cases, since all produced zero post-intervention failures and ER values exceeding 3.0. Only when SEI and DG are added does the assessment differentiate Case B (ER ≥ 4.0 but SEI = 2 and DG = Degrading) from Case A (ER ≥ 4.4, SEI = 1, DG = Permanent). Without this

differentiation, the galvanic boundary in Case B would be under-monitored and the stable geometry in Case A over-monitored. PMPA's three-dimensional structure prevents this conflation by requiring that secondary effects and durability be assessed alongside the primary failure rate reduction.

5.3. Limitations

Preliminary verification covered one case per intervention category in industrial process environments, confirming that Table 1 predictions matched observed outcomes but not establishing the frequency of deviations. Cases where geometry changes produce Degrading outcomes (e.g., gusset corrosion) or material substitutions produce Permanent outcomes (no bimetallic junction) were not represented. SEI's arithmetic summation and the DG reclassification triggers have not been tested against borderline cases. Observation periods (48–84 months) may not capture slow-onset mechanisms such as stress corrosion cracking.

5.4. Practical Implications

PMPA can function as a post-intervention audit tool within maintenance management systems. After an engineering change is implemented, the expected DG from Table 1 serves as a starting hypothesis that defines the initial monitoring protocol: periodic inspection with low frequency for Permanent, interface-focused monitoring with scheduled consumable replacement for Degrading, and parameter-tracking with threshold-based replacement scheduling for Time-limited. Because the expected profile is a prediction rather than a guarantee, monitoring data may contradict it; when a reclassification trigger is met, the protocol escalates to the next category. Encoding these protocols and their escalation rules into a computerized maintenance system would standardize post-intervention follow-up and reduce the risk that a time-limited or degrading intervention is treated as permanent by default.

Conclusions. A Post-Modification Performance Assessment method is proposed as an engineering classification framework for evaluating the long-term

impact of structural changes on mechanical system reliability, rather than as a fully validated predictive reliability model. Three assessment dimensions were defined: effectiveness ratio quantifying failure rate reduction, secondary effect index capturing new degradation mechanisms introduced by the intervention, and durability grade classifying the persistence of the improvement as permanent, degrading, or time-limited. A classification matrix linking intervention type to expected durability profile was constructed, with reclassification triggers for updating the assessment based on monitoring data.

Initial case-based demonstration on three representative industrial cases, each covering a different intervention category, illustrated that the classification logic was consistent with the observed durability outcome in all three instances. Geometry alteration (gusset plate addition) produced a permanent improvement sustained over 84 months with no measurable parameter change. Material substitution (cupronickel tube replacement) eliminated the original failure mode but required active galvanic protection management, matching the degrading profile. Load environment isolation (spring vibration isolators) achieved high initial effectiveness that declined measurably over 48 months due to spring creep, matching the time-limited profile. Comparable primary effectiveness across all three interventions supported the proposition that failure rate reduction alone does not determine long-term reliability trajectory.

Limitations include verification on one case per intervention category, untested borderline scenarios where an intervention deviates from its expected profile, and observation periods that may not capture slow-onset degradation mechanisms. Future work should expand case-based validation across multiple cases per category, develop quantitative thresholds for DG reclassification triggers, and integrate PMPA protocols into computerized maintenance systems for automated post-intervention monitoring.

References

1. Melchers, R. E., & Beck, A. T. (2018). Structural Reliability Analysis and Prediction. 3rd ed. Hoboken, NJ: Wiley.

2. Ang, A. H.-S., & Tang, W. H. (2007). Probability Concepts in Engineering: Emphasis on Applications to Civil and Environmental Engineering. 2nd ed. Hoboken, NJ: Wiley.

3. Fricke, W. (2003). Fatigue analysis of welded joints: state of development. Marine Structures, 16(3), 185–200.

4. Schijve, J. (2009). Fatigue of Structures and Materials. 2nd ed. Dordrecht: Springer.

5. Hobbacher, A. F. (2016). Recommendations for Fatigue Design of Welded Joints and Components. 2nd ed. Cham: IIW/Springer.

6. Ewins, D. J. (2000). Modal Testing: Theory, Practice and Application. 2nd ed. Baldock: Research Studies Press.

7. Harris, C. M., & Piersol, A. G. (2002). Harris' Shock and Vibration Handbook. 5th ed. New York, NY: McGraw-Hill.

8. Fontana, M. G. (1986). Corrosion Engineering. 3rd ed. New York, NY: McGraw-Hill.

9. Roberge, P. R. (2008). Corrosion Engineering: Principles and Practice. New York, NY: McGraw-Hill.

10. Meeker, W. Q., & Escobar, L. A. (1998). Statistical Methods for Reliability Data. Hoboken, NJ: Wiley.

11. Modarres, M., Kaminskiy, M. P., & Krivtsov, V. (2017). Reliability Engineering and Risk Analysis: A Practical Guide. 3rd ed. Boca Raton, FL: CRC Press.

12. Farrar, C. R., & Worden, K. (2012). Structural Health Monitoring: A Machine Learning Perspective. Chichester: Wiley.

13. Jones, D. R. H., & Ashby, M. F. (2019). Engineering Materials 1: An Introduction to Properties, Applications and Design. 5th ed. Oxford: Butterworth-Heinemann.

14. Crow, L. H. (2004). An extended reliability growth model for managing and assessing corrective actions. In Proceedings of the Annual Reliability and Maintainability Symposium (pp. 73–78). IEEE.

15. Rivin, E. I. (2003). Passive Vibration Isolation. New York, NY: ASME Press.